Acta Oceanol. Sin., 2015, Vol. 34, No. 9, P. 23–34
DOI: 10.1007/s13131-015-0720-x
http://www.hyxb.org.cn
E-mail: hyxbe@263.net

The impact of Kuroshio water on the source water of the southeastern Taiwan Strait: numerical results

ZHANG Wenzhou[1, 2, 3*], ZHUANG Xuefen[1, 3], CHEN Chentung Arthur[4, 5], HUANG Tinghsuan[4]

[1] State Key Laboratory of Marine Environmental Science, Xiamen University, Xiamen 361102, China

[2] Coastal and Ocean Management Institute, Xiamen University, Xiamen 361102, China

[3] Fujian Provincial Key Laboratory for Coastal Ecology and Environmental Studies, Xiamen University, Xiamen 361102, China

[4] Department of Oceanography, National Sun Yat-sen University, Kaohsiung 80424, China

[5] Institute of Marine Resources, Zhejiang University, Hangzhou 310058, China

Received 16 March 2015; accepted 29 June 2015

©The Chinese Society of Oceanography and Springer-Verlag Berlin Heidelberg 2015

Abstract

Model output from a Pacific basin-wide three-dimensional physical-biogeochemical model during the period of 1991 to 2008 was used to investigate the impact of Kuroshio water on the source water of the southeastern Taiwan Strait. Based on the characteristic salinities of both Kuroshio water and the South China Sea water, a Kuroshio impact index (KII) was designed to measure the degree of impact. The KII correlates significantly with the northeast-southwest component of wind stress, but the former lags the latter by approximately two months. The correlation coefficient between them increases from 0.267 4 to 0.852 9, with a lag time increasing from 0 to 63 days. The impact of Kuroshio Water is greater in winter and spring than in summer and autumn. At the interannual time scale, El Niño and La Niña events play an important role in impacting the KII. During El Niño events, more Kuroshio water contributes to the source water of the southeastern Taiwan Strait. Conversely, during La Niña events, less Kuroshio water contributes to the source water.

Key words: Kuroshio water, seasonal variation, interannual variation, Taiwan Strait

Citation: Zhang Wenzhou, Zhuang Xuefen, Chen Chentung Arthur, Huang Tinghsuan. 2015. The impact of Kuroshio water on the source water of the southeastern Taiwan Strait: numerical results. Acta Oceanologica Sinica, 34(9): 23–34, doi: 10.1007/s13131-015-0720-x

1 Introduction

The Taiwan Strait (TWS), which has a mean depth of approximately 60 m, is adjacent to the South China Sea (SCS) and the Luzon Strait (LS) to the south and the East China Sea to the north (Fig. 1). There is a deep submarine canyon known as the Gaoping Submarine Canyon in the southeastern TWS, tapering from south to north. This canyon is surrounded by the broad continental shelf of Mainland China, the deep SCS basin, and Taiwan Island. Kuroshio water (KW) often intrudes into the TWS through this canyon (Hu et al., 2010; Jan et al., 2010). The source water at the south gate of the southeastern TWS is controlled by the circulations in the northeastern SCS and the TWS, including Kuroshio intrusion current through the LS.

Circulations in the northeastern SCS and its adjacent straits have been extensively investigated in the past (e.g., Hu et al., 2000; and references therein). The SCS is in the East Asian monsoon regime, where northeasterly winds prevail in winter but southwesterly winds prevail in summer. Forced by monsoon winds, overall seasonal circulation in the SCS is cyclonic in winter and anti-cyclonic in summer (Chu et al., 1999; Hu et al., 2000). As one part of the overall seasonal circulation, the seasonally averaged current in the northeastern SCS is westward or southwestward in winter and is eastward or northeastward in summer. However, the circulation in the northeastern SCS shows a more complex pattern and greater variability than the above general features because of Kuroshio intrusion through the LS, as well as the influence of topography.

The Kuroshio current, which has high temperature and salinity, originates from the North Equatorial Current at approximately 10° to 15°N and flows northward along the eastern Philippine coast. When the Kuroshio passes by the LS, the KW frequently enters the SCS in the forms of a branch, a loop, or shed eddies (Caruso et al., 2006; Liang et al., 2008; Yuan et al., 2008; Jan et al., 2010; Nan et al., 2011a). Although most of the KW entering the SCS flows back to the main stream of the Kuroshio, some may intrude into the SCS and the TWS (Hu et al., 2010).

In winter, a branch of the Kuroshio often flows northwestward through the LS into the northeastern SCS and later turns to the west along the continental slope. This branch is called the SCS branch of Kuroshio. A portion of the branch water may separate from the branch and intrude into the southeastern TWS through the Gaoping Canyon and later flow northward along the

Foundation item: The National Natural Science Foundation of China under contract Nos 41076002 and 41276007; the Fundamental Research Funds for the Central Universities under contract Nos 2010121036 and 2013121047; the Joint Fund Program for Promoting Science & Technology Cooperation across the Taiwan Strait supported by the National Natural Science Foundation of China and Fujian Province under contract No. U1305231.

*Corresponding author, E-mail: zwenzhou@xmu.edu.cn

west coast of Taiwan Island (Jan et al., 2010). In summer, the Kuroshio flows first through the LS, then moves along an anticyclonic loop in the northeastern SCS, lastly returns to the east of the LS. This pattern is called the Kuroshio's Loop Current (e.g., Caruso et al., 2006; Hu et al., 2010). Some KW leaving the loop current heads northward to the eastern part of the TWS. However, some studies show that the intrusion of the KW into the northeastern SCS is accomplished through transient events, rather than a persistent circulation (e.g., Yuan et al., 2006; Nan et al., 2011a). Branch currents are a dominant intrusion pattern in winter, whereas loop currents appear more frequently in summer (Yuan et al., 2006). For a full year, the likelihood of occurrence of the loop pattern is slightly higher than that of the branch pattern (Nan et al., 2011a). During 1992–2001, anticyclonic eddies intermittently shed from the Kuroshio current and moved into the northeastern SCS in both winter and summer monsoon periods (Li et al., 1998; Jia and Liu, 2004), which may have also affected the source water of the southeastern TWS during this period.

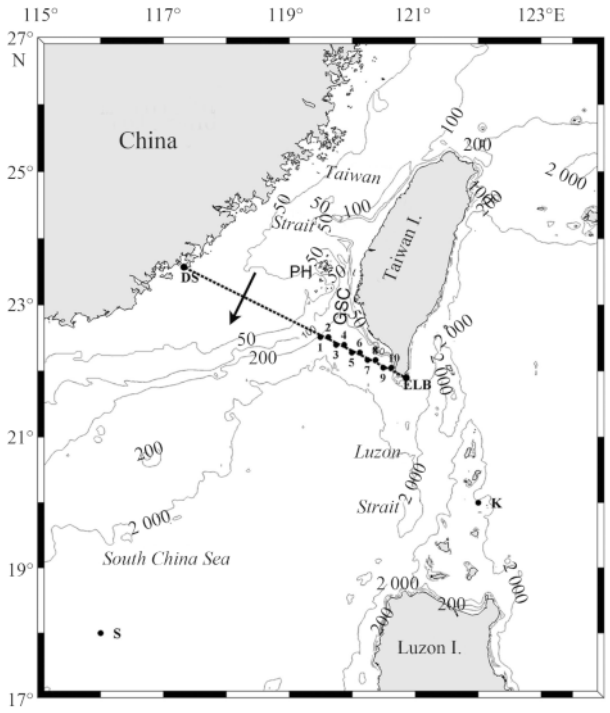

Fig. 1. Study area and bathymetry. Gray contours are isobaths in meters. The dashed line shows the section across the Taiwan Strait with two ends: Dongshan (DS) to the west and Eluanbi (ELB) to the east. Ten stations numbered on the section are aligned evenly along the south gate of the southeastern Taiwan Strait, where the water depth is larger than 200 m. Black arrow marks the positive direction of the wind stress component normal to the section. PH and GSC denote the Penghu Islands and Gaoping Submarine Canyon, respectively.

The intrusion of the Kuroshio into the TWS has been the subject of much discussion over the last twenty years (e.g., Chuang, 1985; Jan et al., 2002; Chen et al., 2010). Based on two current meter moorings deployed in the TWS, Chuang (1985) speculated that the mean flow in the TWS probably originates from branching of the Kuroshio through the LS. Jan et al. (2002) combined hydrography data and satellite sea surface temperature images with a numerical model to study the seasonality of circulations in the TWS. These researchers found that the Kuroshio branch water (KBW) is bounded in the Penghu Channel and blocked by strong northeast monsoon in winter. With the weakened northeast monsoon in spring, the once bounded KBW in the Penghu Channel flows northward and consequently covers the entire eastern part of the TWS. In summer and autumn, the KBW in the Penghu Channel is replaced by the SCS water (SCSW). From the results of cluster analysis, Jan et al. (2006) found that the KBW exists persistently in the southeastern TWS throughout the year. Using field observations and a numerical model, Chen et al. (2010) demonstrated that the Kuroshio did not intrude into the southern TWS in the spring of 2008, when the TWS was under the influence of La Niña. Although most of the investigations mentioned above confirm the impact of the Kuroshio on water in the TWS, its seasonal and interannual variability is still unclear. Additionally, the KW usually mixes with other waters, such as the SCSW, before and after it intrudes into the TWS. Therefore, it does not keep all the properties associated with the KW as the Kuroshio branch current conventionally described. For these reasons, the purpose of this work is to examine the seasonal and interannual variability of the impact of the KW on the source water of the southeastern TWS because the KW intrudes into the TWS mainly through this mechanism.

The rest of this paper is organized as follows. The model and data used in this work are described in Section 2. In Section 3, a simple index is designed to quantitatively evaluate the impact of the KW on the source water of the southeastern TWS. Section 4 demonstrates the seasonal and interannual variations of the impact, and discusses its relationship with monsoon winds and El Niño/La Niña events. The results are summarized and conclusions presented in the last section (Section 5).

2 Model and data

The original data used in this study were output from a three-dimensional physical circulation model for the Pacific Ocean (45°S to 65°N, 99°E to 70°W), which was based on the Regional Ocean Model System (ROMS), referred to as the Pacific ROMS model. The ROMS is a free-surface, hydrostatic, primitive equation ocean model utilizing orthogonal curvilinear coordinates in the horizontal and a topography-following coordinate in the vertical. Wang and Chao (2004) first developed the Pacific ROMS model at a resolution of 50 km in the horizontal and 20 levels in the vertical. Xiu et al. (2010) increased its resolution to 12.5 km ((1/8)°×(1/8)°) and 30 levels for the entire Pacific Ocean domain. A sponge layer with a width of 5° from the northern and southern boundaries of the model was set for temperature, salinity, and nutrients. To restore the modeled temperature, salinity, and nutrients to observations at the two boundaries, three delay terms were separately added to the sponge layer in the temperature, salinity, and nutrient equations. The model was initialized with climatological temperature and salinity from the World Ocean Atlas 2001 and forced with the climatological air-sea fluxes from the NCEP/NCAR reanalysis (Kalnay et al., 1996) over decades to reach quasi-equilibrium. Subsequently, the blended daily sea wind (Zhang et al., 2006) and daily air-sea fluxes of heat and freshwater from the NCEP/NCAR reanalysis (Kalnay et al., 1996) were used in the model for the period 1991–2008. The freshwater flux through air-sea interface was taken into account by precipitation and evaporation; however, river discharges were not included in this model. The model has been described in more de-

tail by Xiu et al. (2010). Three-day averaged data were saved and used in this study. The output from this model has been validated and applied in several analyses of the SCS (e.g., Xiu et al., 2010; Nan et al., 2013). For example, Nan et al. (2013) applied the output data of this model to investigate variation of the Kuroshio intrusion into the SCS. Their study area is similar to the one used in this analysis. They found that the correlation coefficient of monthly geostrophic transports between the model results and satellite remote sensing observations is 0.77 with a significance level above 95%, and 0.87 for the interannual variation.

3 Methods

3.1 *Kuroshio impact index (KII)*

As the Kuroshio intrudes into the SCS through the LS, it often entrains and mixes with the SCSW. After the KW incidentally flows into the TWS, it appears as the mixture of the KW and the SCSW, with water properties between them. Based on the water properties, we attempt to analyze the impact of the KW on the water source of the southeastern TWS.

When two water masses with different temperatures mix together, the resultant water temperature is difficult to determine. Additionally, water temperature is markedly influenced by air-sea interaction, sunlight cycle, and the presence of land masses. Compared with temperature, the salinity of seawater is relatively conservative, although at the surface it may be affected by freshwater flux and river discharges. Additionally, the total content of salt does not change when two water masses with different salinities meet. Thus, the salinity is fittingly taken as an indicator used to reveal the relative proportion in the mixture of two waters. The Kuroshio intrusion into the southeastern TWS originates from a deep canyon where the water depth exceeds 200 m (Jan et al., 2010). To avoid the influence from freshwater flux and river discharge, the seawater at the layer of 200 m deep is used. Based on the conservation of salt contained in seawaters, a Kuroshio impact index (KII) is designed as follows,

$$KII = \frac{X - S}{K - S}, \tag{1}$$

where S is the salinity at 18°N, 116°E (Point S in Fig. 1), representing the SCSW; K is the salinity at 20°N, 122°E (Point K in Fig. 1), representing the KW; and X is the salinity at Stas 1–10 that evenly align along a cross-strait section at the gate of the deep canyon in the southeastern TWS (Fig. 1). The KII represents the proportion of the KW to the mixed seawater, indicating the impact of KW on the source water of the southeastern TWS based on the hypothesis that the seawater there is only the mixture of the SCSW and the KW. The KII ranges from 0 to 1. When it equals 1, the seawater is composed of the KW only. Conversely, when it equals 0, the seawater is composed of SCSW only. Figure 2 shows the time series of monthly mean KII from 1991 to 2008, calculated from the model output data described above.

3.2 *Ensemble empirical mode decomposition (EEMD)*

As an adaptive and highly efficient method for analyzing nonlinear and non-stationary data, the empirical mode decomposition (EMD) method developed by Huang et al. (1998) has been applied to many scientific fields, such as physical oceanography (e.g., Lai and Huang, 2005). This method is able to decompose any complicated data into a finite, physically meaningful intrinsic mode functions (IMFs) applied to linear and nonlinear processes. Each IMF satisfies two conditions: (1) the number of extrema and the number of zero crossings must be equal or differ by one; (2) the mean value of the upper and lower envelopes connecting all local maxima and minima, respectively, is zero at any data point.

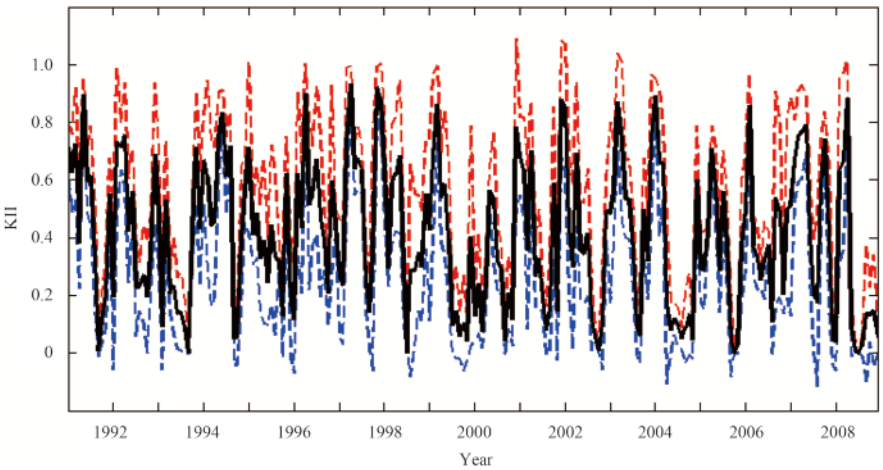

Fig. 2. The time series of monthly mean KII (solid curve) during the period from 1991 to 2008. Red and blue dashed curves denote one standard deviation above and below monthly mean KII, respectively. The standard deviation is calculated separately for every month.

As described by Huang et al. (1998), the procedure of the EMD method can be simply presented as follows: (1) identifying all local maxima and minima of a data series; (2) connecting all maxima and all minima with two cubic spline lines separately to obtain the upper and lower envelops of the data series; (3) calculating the mean of the upper and lower envelops; (4) repeating Steps (1)–(3) on the difference (residual) between the data and the mean if the residual does not satisfy the two conditions of the IMF; (5) if the residual almost satisfies the two conditions of the IMF, it is regarded as an IMF (one component); taking the difference between the data series and this component as a new data series and repeating the above steps on it until all IMFs (components) residing in the original data series are obtained.

There are several disadvantages of the EMD, such as mode

mixing (Wu and Huang, 2009). To overcome its drawbacks, an ensemble EMD (namely EEMD) has been designed by Wu and Huang (2009). Superposing a uniformly distributed white noise on original data, the signals with different scales in the data are projected onto proper scales established by the white noise background. The EEMD is attempted multiple times by inputting different white noises into the same original data. For each trial, a random white noise with the same amplitude is superposed on the original signal. The final IMFs are obtained by averaging the corresponding IMFs from all trials. Meanwhile, all white noises are canceled out because of their statistical characteristics (Wu and Huang, 2009).

Two parameters are required when the EEMD is applied: the ratio of the standard deviation of added noise to that of original data (Nstd) and the ensemble number or the number of trials (NE). Wu and Huang (2009) suggested that the Nstd should be 0.2 and the NE should be a few hundred for a good result. Palacz et al. (2011) set the Nstd and NE to be 0.1–0.2 and 500–700, respectively, when they applied the EEMD in examining the seasonal and interannual changes of surface chlorophyll in the SCS.

To improve the IMFs from the EEMD further, post-processing is necessary. Wu and Huang (2009) presented a post-processing approach by applying the EMD to the IMFs from the EEMD. After obtaining all modified IMFs using the EMD, the final residual would be taken as the trend of the original signal. For every IMF, the number of zero-crossings and extrema should be the same or differ by only one. In addition, a physically meaningful IMF must be statistically significant, with a prescribed significance level (e.g., 95% or 99%). In this study, the monthly mean KII based on the model results, monthly mean blended sea surface wind data (Zhang et al., 2006), and monthly Oceanic Nino Index (ONI, http://www.cpc.ncep.noaa.gov/products/analysis_monitoring/ensostuff/ensoyears.shtml) were analyzed using the EEMD following the methods presented by Wu and Huang (2009).

4 Results and discussion

Figure 2 shows that the KII time series exhibits obvious seasonal and interannual variations superposed by small inter-seasonal variations. The impact of KW on the source water of the southeastern TWS, indicated by the KII, depends on the circulations in the northeastern SCS and TWS, particularly the pattern of the Kuroshio intrusion into the SCS through the LS. These circulations are not only regulated by the conditions of large scale winds and circulations, but also influenced by mesoscale processes such as mesoscale eddies (e.g., Wang et al., 2008; Zhuang et al., 2010; Zu et al., 2013). These mesoscale processes play an important role in the momentary and inter-seasonal variations of the circulations. Since this work focuses on the seasonal and interannual impacts of KW, the influence of these mesoscale processes was not considered separately. However, their net contribution, if there is one, may be included implicitly and statistically in the seasonal and interannual variations of the KII.

4.1 *Seasonal impact*

Figure 3 shows multi-year averaged seasonal KII values at the ten stations shown in Fig. 1. It is noted that the values of the KII in the middle of the ten-station section are larger than those at the two ends, indicating that the KW intrudes into the southeastern TWS mainly through the middle of this section. There is a seasonal difference in the KII for all stations. The KII is larger in winter (December to February) and spring (March to May) than in summer (June to August) and autumn (September to November). This means the KW has a greater contribution to the source water of the southeastern TWS in winter and spring than in other seasons. On average, the KW is comparable to the SCSW in

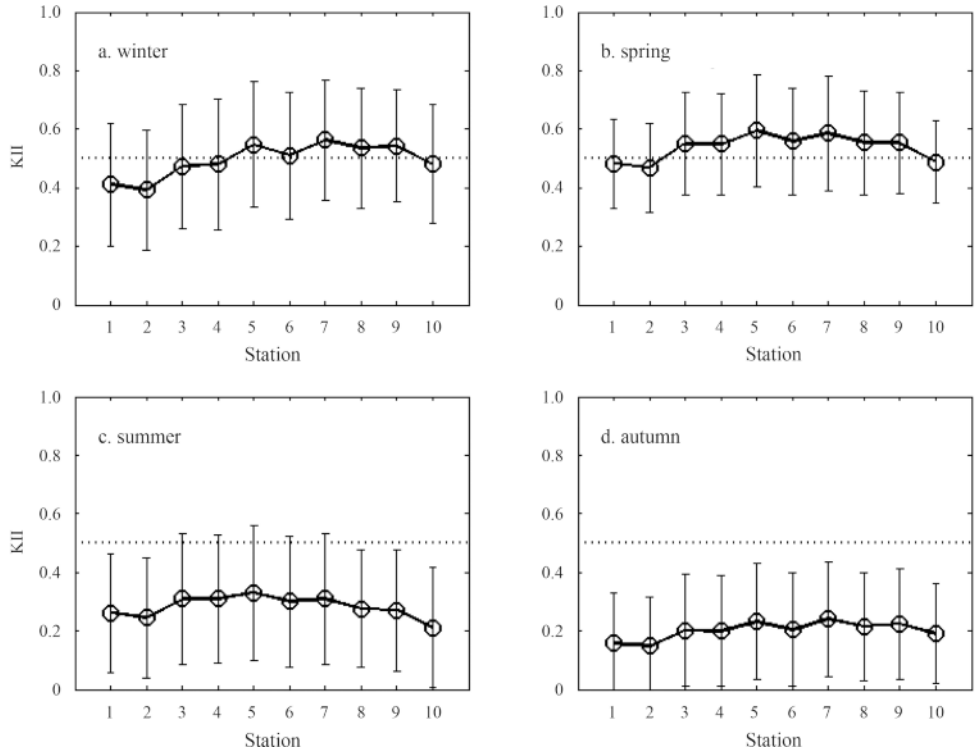

Fig. 3. Multi-year averaged seasonal KIIs at the ten stations that are shown in Fig. 1. Error bars show one standard deviation away from the averaged values.

winter, but slightly dominates in spring, with the KII above 0.5 averaged along the section. However, this is not the case for an individual year given that the KII values are dispersive and have a large standard deviation. By contrast, the SCSW is overwhelming in summer, particularly in autumn because the KII during this period is generally smaller than 0.5. These results are consistent with historical current measurements and hydrographic data obtained in the eastern TWS. As summarized from these observations by Wang and Chern (1988), northeastward-flowing KW frequently appears in the eastern strait during winter and lasts to spring, sometimes even through early summer. Thereafter, the SCSW floods into the TWS and the KW stops entering with the onset of southwest monsoon. Recent observations and numerical simulations support that while the water in the TWS originates from the SCSW in summer, it probably comes from the KBW in winter (Jan et al., 2010).

The above results suggest that the seasonal change of the KII may be associated with the activity of northeast and southwest monsoon winds. It is well known that the Kuroshio westward intrusion through the LS, as well as the circulations in the northeastern SCS, is modulated by monsoon wind forcing (Hu et al., 2000; Yuan et al., 2014). The seasonal variation of the Kuroshio intrusion is closely related to the East Asian Monsoon winds (Yuan et al., 2014). The Kuroshio intrusion is strongest in winter, when northeast monsoon wind prevails. In contrast, the Kuroshio stops intruding into the SCS in summer, when southwest monsoon wind takes the place of northeast monsoon wind. Additionally, northeast and southwest monsoon winds regulate the circulations in the TWS and adjust the intrusion of KW into the strait (Jan et al., 2002, 2006; Hu et al., 2010; Jan et al., 2010). To the best of our knowledge, however, the detailed relationship between monsoon wind forcing and the impact of the KW on the source water of the southeastern TWS has not been historically documented in the literature and remains unclear.

Since the prevailing wind in the study area is southwestward in winter and northeastward in summer, the principal axis of the wind is along the southwest-northeast orientation, which is approximately perpendicular to the section mentioned previously. Therefore, only the component of wind stress normal to the section (referred as to DWS) was used to check its relationship with the KII, as shown in Fig. 1. The wind stress is averaged over the study sea area. The positive DWS is defined southwestward and the negative is defined northeastward. Figure 4 shows the multi-year (1991–2008) averaged year-round three-day average DWS and KII. The northeast wind begins in autumn, becomes strongest in winter, and decays in spring. The southwest wind only prevails in summer. It is noted that at an annual time scale, the KII changes nearly in phase with the DWS, but with an obvious time lag between them. The correlation coefficient (R) between the KII and the DWS is 0.267 4, with a significance level of 99%. Generally speaking, the northeast monsoon wind creates favorable conditions for the appearance of KW, whereas the southwest monsoon wind creates unfavorable conditions. The time lag between wind and the KII can be observed from the seasonal evolution of the KII in Fig. 3. The KII is largest in spring, with a mean value of 0.51, but weakest in autumn, with a mean of 0.18, lagging wind evolution by one season. To obtain more accurate information about the time lag, a time-lag correlation analysis was conducted for the above KII and DWS. Figure 5a displays the change of the R between the KII and the DWS versus time lag. The R increases monotonously from 0.267 4 to 0.852 9 when the lag time is prolonged from zero to 63 days (about two months). When the KII is shifted forward by 63 days, it matches well with the DWS (Fig. 5b). Using the time series of monthly mean KII and DWS from 1991 to 2008 instead of the above multi-year averaged three-day average values, a similar correlation analysis shows that the R between them changes from 0.102 4 to 0.445 6, with a significance level of 90% when the KII is shifted forward by two months (figure omitted).

Seasonally averaged wind stress and modeling sea surface level (SSL) with currents at 200 m deep are shown in Fig. 6. The currents are almost parallel to SSL contours, indicating the dominant effect of geostrophic balance on the currents. The alternation

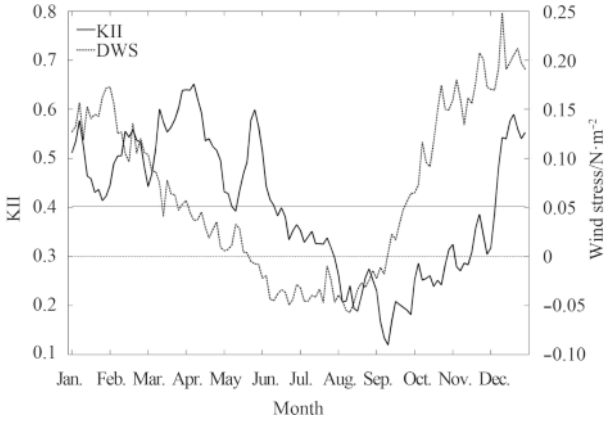

Fig. 4. Multi-year averaged annual variations of the KII and wind stress (DWS) based on three-day averaged data. Gray solid and dot-dashed lines denote the mean of the KII and zero for the DWS, respectively.

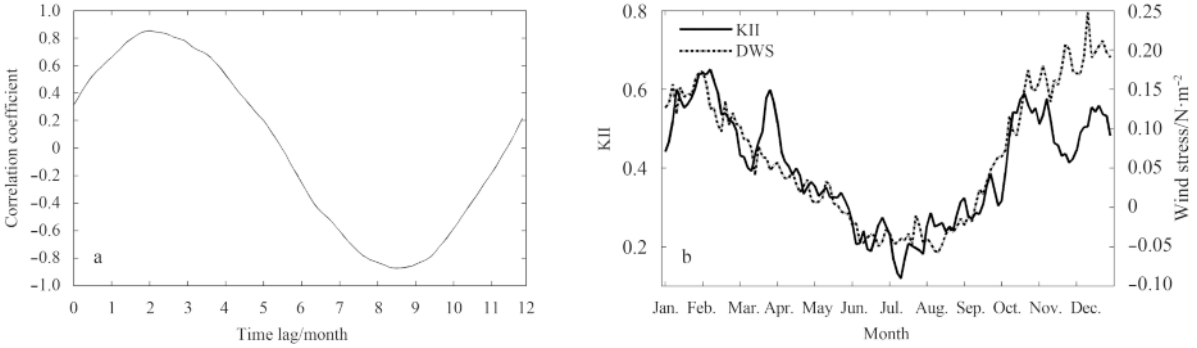

Fig. 5. Relationship between the annual KII and DWS averaged during the period from 1993 to 2008 based on three-day averaged data: a. the correlation coefficient versus time lag; and b. two time series after the KII is shifted forward by 63 days.

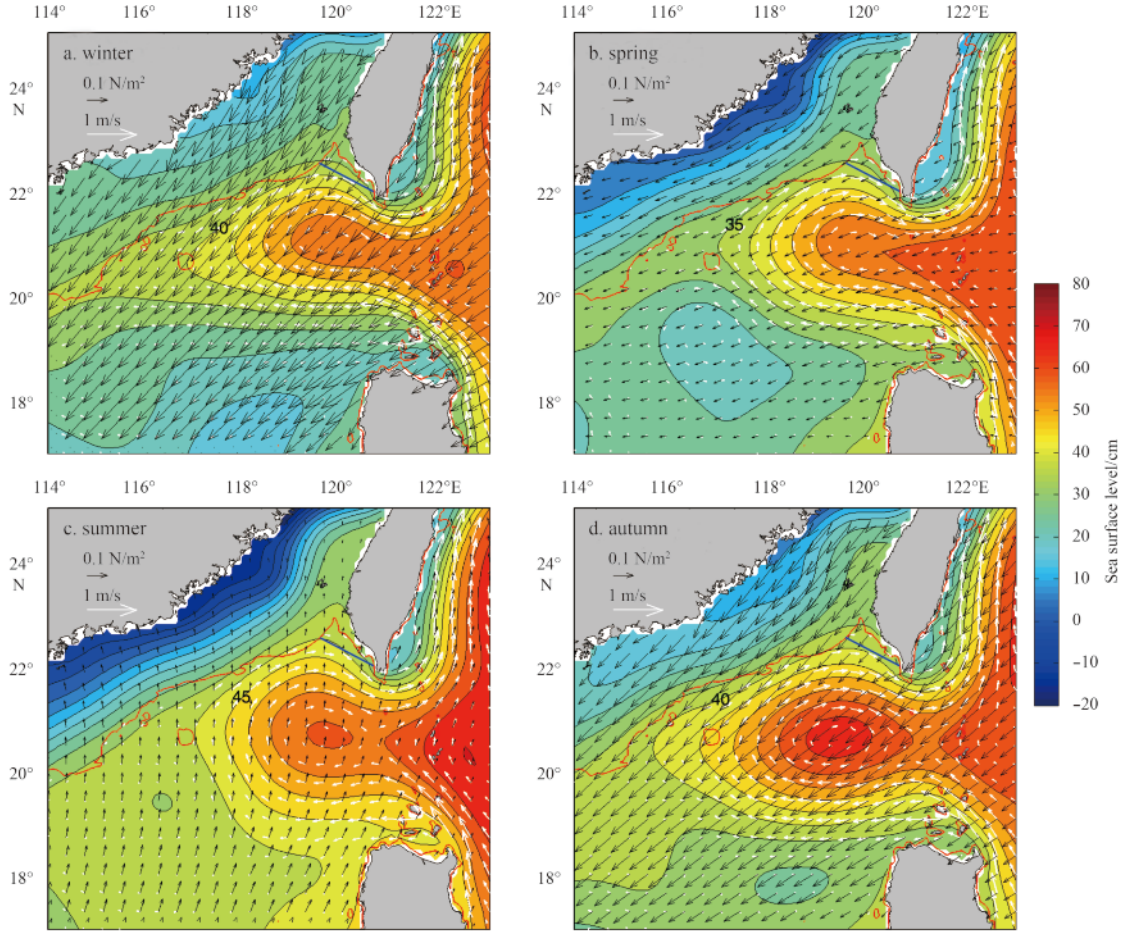

Fig. 6. Seasonal mean wind stress (black arrows) at 10 m above the sea surface and modeling sea surface level (colors with contours) with currents (white arrows) at 200 m deep. The interval of the contours is 5 cm. Red curves denote the isobath of 200 m and blue line indicates the location of the section described in Fig. 1. The contour denoted by a number indicates the west edge of the mean Kuroshio loop, suggesting that the seawater east of this contour originates mainly from the Kuroshio water.

of northeast and southwest monsoon winds affects the seasonal distribution of the SSL and then modulates the currents. Figure 6 shows that the west boundary of the northward-flowing Kuroshio, characterized by strong SSL zonal gradient, is very distinct, extending from east of Luzon Island to east of Taiwan Island.

In winter, northeast monsoon wind drives water, via Ekman transport, to flow toward the western bank in the TWS, which reduces the eastward cross-strait SSL gradient. In the LS, the northeast wind intensifies the Kuroshio intrusion into the northeastern SCS. There is a very low SSL area to the northwest of Luzon Island. A cyclonic circulation, called the Northwest Luzon Cyclonic Gyre, is formed around the low SSL area (Hu et al., 2000). A part of the KW flows westward as one part of the cyclonic circulation. Still, some KW may intrude into the southeastern TWS in the form of a loop because a tongue of SSL extends into the southeastern TWS. The SSL contour of 40 cm starting from the Kuroshio current east of Luzon Island is very close to the section at the south gate of the southeastern TWS. Because of the blocking of southwestward wind, the KW permeating the southeastern TWS hardly goes through the strait. From simulated currents and drifter trajectories, Jan et al. (2010) postulated that although the KBW rarely flows into the TWS in winter, the westward movement of the Kuroshio brings high salinity water to the southeastern TWS along a loop route.

In spring, the decay of northeast wind (Figs 6b and 4) permits the KW in the southeastern TWS to flow northward. Based on the hydrography data, Jan et al. (2002) found that the weakened northeast monsoon in spring allows the KBW to flow northward and cover the entire eastern TWS. At the same time, the low SSL area northwest of Luzon Island becomes weaker with the sea level rising and expands northward, resulting in a moderate SSL south-north gradient and a weak westward current. These cause massive KW to easily intrude into the southeastern TWS. The SSL contour of 35 cm at the western edge of the Kuroshio stretches into the southeastern TWS north of the section, indicating the intrusion of the KW. The above two aspects are the main reasons why the KII lags the DWS as described previously.

In summer, southwest and south winds instead of northeast wind prevail in the study area (Fig. 6c). On the continental shelf of the northern SCS and in the TWS, the gradient of the SSL is obviously intensified and directs southeastward. These are favorable conditions for the SCSW to flood into and flow through the TWS. The eastward movement of the SCSW and southwest wind impede the intrusion of the Kuroshio into the northeastern SCS. The main part of the Kuroshio secedes from the LS and directly flows northward to the east of Taiwan Island. Only a part of the KW leaks into the SCS as a loop and sheds as eddies from the Kuroshio. Additionally, the Kuroshio current becomes strongest

in summer and then tends to leap the LS (Sheremet, 2001). Weak SSL gradient across the LS also prevents the KW from entering the northeastern SCS, as a great SSL cross-strait gradient in the LS is the main factor to induce the Kuroshio intrusion (Qu, 2000; Liang et al., 2008). Figure 6c shows that the west envelope curve of the Kuroshio loop denoted by the SSL contour of 45 cm is separated from the section southwest of Taiwan Island by the water originating mainly from the SCS. As a result, relatively low salinity water of the SCS flows into the southeastern TWS, replacing high salinity KW.

In autumn, due to the onset of northeast monsoon wind, an SSL pattern similar to that in winter begins to appear in the TWS (Figs 6d and 4). The northeast wind is not very strong in autumn and the Kuroshio requires some time to slow down enough before it largely intrudes into the SCS (Sheremet, 2001). Although the west edge of the Kuroshio loop, denoted by the 40 cm SSL contour, comes very close to the section at the southeastern TWS, the KW travels a longer distance along the edge in the SCS and has more chance to mix with the SCSW than that in winter. Thus, the SCSW dominates in the southeastern TWS and the impact of the KW on its source water is very weak in autumn.

As known from the results and discussion presented above, northeast wind is favorable for the Kuroshio intrusion into the SCS through the LS, providing the KW for the southeastern TWS; on the other hand, the northeast wind in the TWS blocks the KW from flowing northward through the TWS. The value of the KII is determined by the competition between these two effects of northeast wind. On the seasonal timescale, the former is dominant over the latter, resulting in a positive correlation between the wind stress and the KII. Nevertheless, the latter causes the phase of the KII to lag that of the wind stress by about two months. Additionally, it is noted that the KII exhibits more evident inter-seasonal variations than the TWS in the first half year (Fig. 4), indicating the inconsistency between them at the smaller time scale than the seasonal.

Both numerical model simulations and satellite observations revealed that the Kuroshio intrusion into the SCS manifests as transient events, including eddy shedding, rather than as a persistent phenomenon (Yuan et al., 2006; Nan et al., 2011a). Figure 7 shows the distribution of the standard deviation of the SSL for every season, which reflects the variability of the SSL associated with such events. It is obvious in Fig. 7 that the variability of the SSL southwest of Taiwan Island is smaller in autumn than in other seasons. Using a high-resolution numerical model, Tsui and Wu (2012) found that Kuroshio intrusion events happen more frequently in winter than in summer. Yuan et al. (2006) demonstrated from satellite remote sensing data that winter is the most favorable for the Kuroshio anticyclonic intrusions but there are more episodes of the intrusion in summer than in winter. Nan et al. (2011b) demonstrated that summer and winter are the favorite seasons for eddy formation southwest of Taiwan while the fewest eddies are generated there in autumn. In winter and summer, the large standard deviation extends southwestward in a band pattern along the continental slope, which may be related

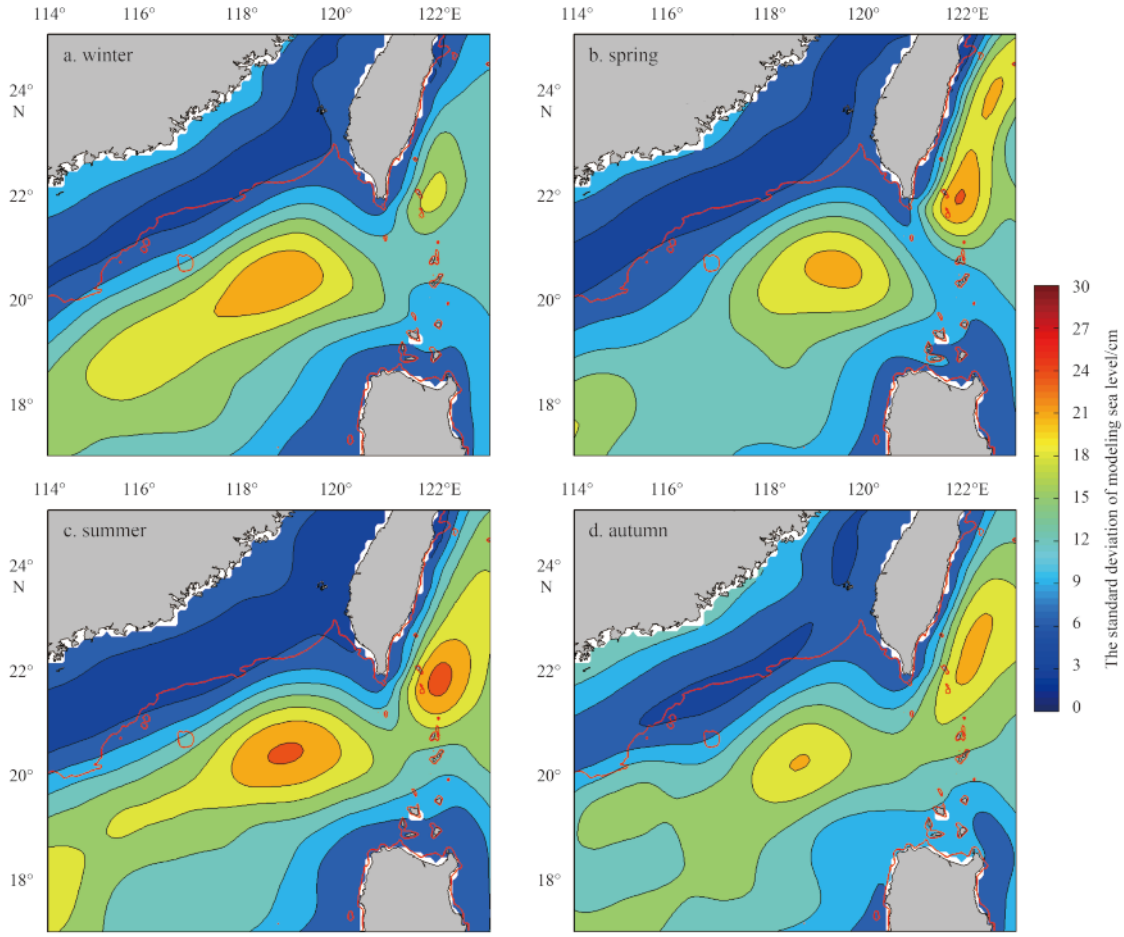

Fig. 7. The standard deviation of modeling sea level for every season. The interval of contours is 3 cm. Red curves denote the isobath of 200 m.

to the eddies shedding from the Kuroshio. Yuan et al. (2006) showed that anticyclonic eddies shedding from most anticyclonic intrusions of the Kuroshio usually move along the continental slope of the northern SCS to the west. The weakest variability of the SSL seemingly corresponds to the smallest KII in autumn. Although the change of the KII is basically consistent with the variability of the SSL in autumn, winter and spring, the inconsistency between the strongest SSL variability and the small KII in summer suggests that frequent transient events not always contribute much to the seasonal impact of the KW on the source water of the southeastern TWS.

4.2 *Interannual impact*

To obtain the interannual variation, the EEMD analysis described previously was applied to the monthly mean KII time series from 1991 to 2008. The KII (input) and its components (C1–C6 and residual) are shown in Fig. 8a. The last component is the residual and the others are the IMFs. Most IMFs, except C4 and C6, are statistically significant, with a significance level of 95% (Fig. 8b). C3 denotes the seasonal, or annual, variation, as it has an average period of approximately one year. C4–C6 have a mean period of 2.2, 4.4, and 7.4 years, respectively, indicating interannual variations. As only C5 is significant with a level higher than 95%, the interannual variation represented by C5 will be the focus.

The peaks of C5 appear in 1991, 1994, 1997, 2002 and 2007, whereas the troughs occur in 1992, 1995, 1999–2000, 2004–2005, and 2008 (Fig. 8a). Some sparse and intermittent *in situ* observations and satellite remote sensing data have indicated that the interannual difference of Kuroshio intrusion water in the TWS seems to be associated with monsoon winds and El Niño/La Niña events (e.g., Shang et al., 2005; Chen et al., 2010). However, the relationships at the interannual time scale between source water from the south in the southeastern TWS and both monsoon winds and El Niño/La Niña events have not been presented in detail at this time. To examine the relationships, we analyzed monthly DWS and ONI using the same method as the KII. The results are shown in Fig. 9. Among the IMFs of the DWS, the seasonal component (C2) is the most significant, implying that the seasonal band is overwhelming in the variations of monsoon winds. The interannual band in the DWS includes the contributions from the components C3, C4, and C5. However, C4 is more significant than the other two components. It has an average period close to that of the C5 component of the KII. By contrast, all IMFs of the ONI except C1 are significant, with a significance level of 99%. Both C4 and C5 components exhibit the interannual variations of the INO, but C4 has an amplitude (above 0.5) larger than that (below 0.5) of C5 (Fig. 9b). We therefore chose C5 of the KII (KII-C5), C4 of the DWS (DWS-C4), and C4 of the ONI (ONI-C4) to analyze the connections between their interannual variations, not only because they best represent their interannual variations, but also because they have comparable average periods.

For comparison, Fig. 10 shows the time series of KII-C5, DWS-C4, and ONI-C4 together. It is interesting that KII-C5 is almost in phase with ONI-C4, but out of phase with DWS-C4. Correlation

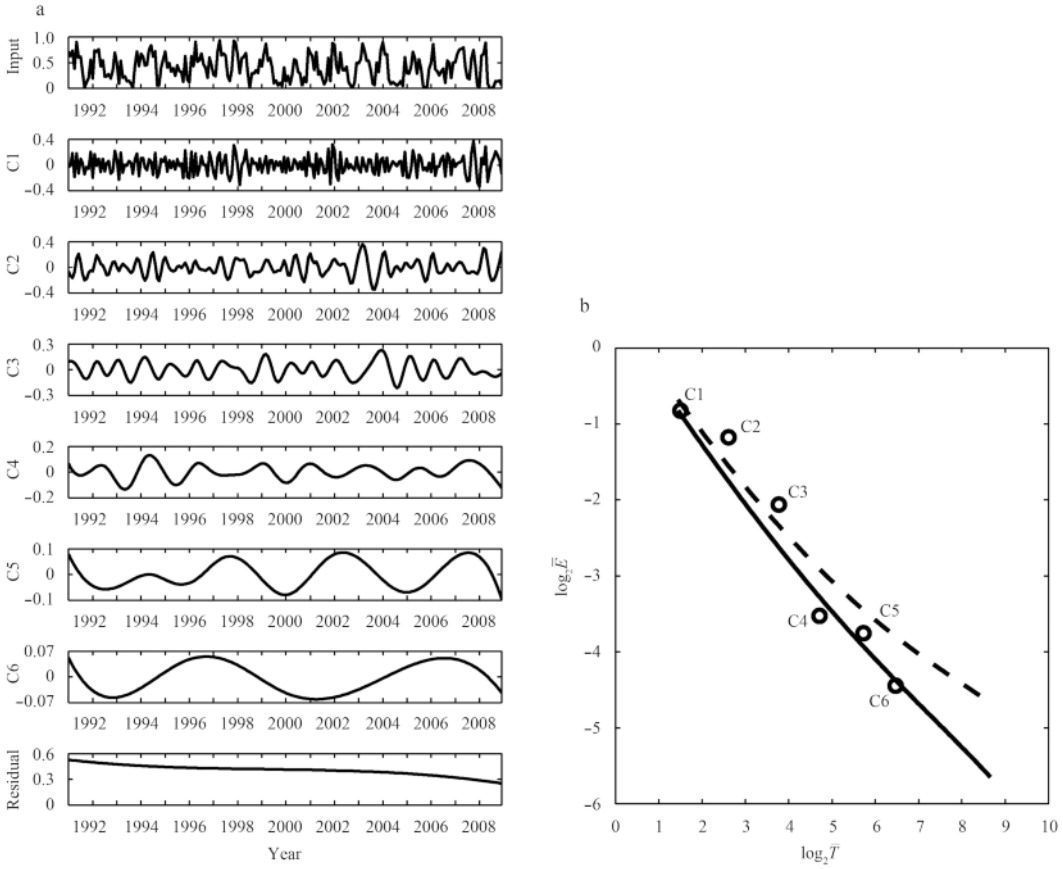

Fig. 8. Decomposition of the KII using the EEMD method. a. The monthly mean KII (input) and its components (C1–C6 and residual) and b. statistical significance tests for the components (C1–C6) with 99% (dashed line) and 95% (solid line) significance levels. In Fig. 8b, T is the mean period (months) and E is the mean normalized energy.

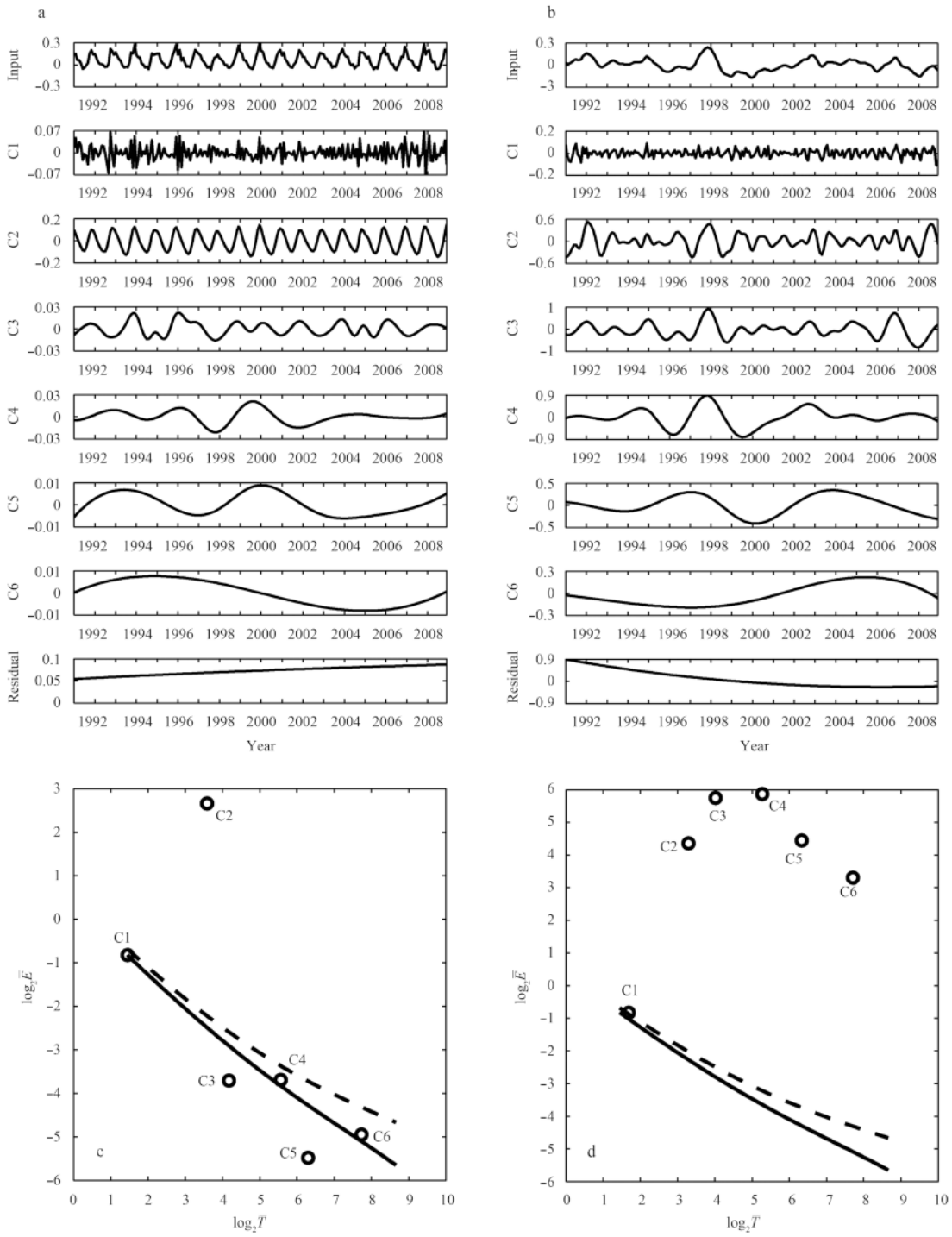

Fig. 9. The same to Fig. 8 but for the monthly DWS (a, c) and ONI (b, d).

analyses demonstrate that the correlation coefficient between KII-C5 and ONI-C4 is 0.630 3, and that between KII-C5 and DWS-C4 is –0.755 1. Both correlations are significant, with a significance level of 99%. Note that the peaks and troughs of KII-C5 are almost consistent with the highest and lowest values of ONI-C4, but with the minimum and maximum values of DWS-C4, respectively. The peaks of ONI-C4 coincide with the El Niño events happening during the period from 1991 to 2008, while its troughs coincide with the La Niña events, as do those of KII-C5. During the El Niño events, a higher KII-C5 value indicates a greater impact of KW on the water at the south gate of the southeastern TWS, while a smaller DWS-C4 value reflects weakness of northeast wind or enhancement of southwest wind in the study area. During the La Niña events, a lower KII-C5 value means less impact from KW and a larger DWS-C4 value implies enhancement of northeast wind or weakness of southwest wind.

The interannual variability of circulations in the study area is mainly determined by the interannual variations of the East Asian monsoon winds and Kuroshio intrusion into the SCS (Caruso et al., 2006). The strong northeast winter wind blocks the Kurosh-

io intrusion into the TWS, while the weak northeast wind allows the KW to flow northward through the TWS (Jan et al., 2006; Hu et al., 2010; Wu and Hsin, 2012). The East Asian monsoon winds not only directly regulate the source water of the southeastern TWS by driving the circulations in the northeastern SCS and TWS, but also indirectly affect it by modulating the Kuroshio intrusion into the SCS through the LS. By evaluating the relationship between wind stress and Kuroshio intrusions into the SCS in the winters of 1999–2005, Caruso et al. (2006) demonstrated that southern (northern) intrusions in the LS are associated with stronger (weaker) wind stress curl fields. The intrusion pattern in the northeastern SCS is affected by the latitudinal position of the intrusion in the LS. Southern intrusions typically produce long-lived anticyclonic loop currents, whereas northern intrusions typically form short-lived weak cyclonic circulations. Numerical experiments by Wu and Hsin (2012) show that the variations of Kuroshio intrusion through the LS are closely related to wind and that the wind stress curl southwest of Taiwan Island plays a particularly important role. The above effects of wind on the source water of the southeastern TWS are too complex to be identified separately. Figure 10 suggests that at the interannual time scale abnormally strong (weak) northeast wind enhances (reduces) its blocking effect in the TWS, which is unfavorable (favorable) for the KW contributing to the source water.

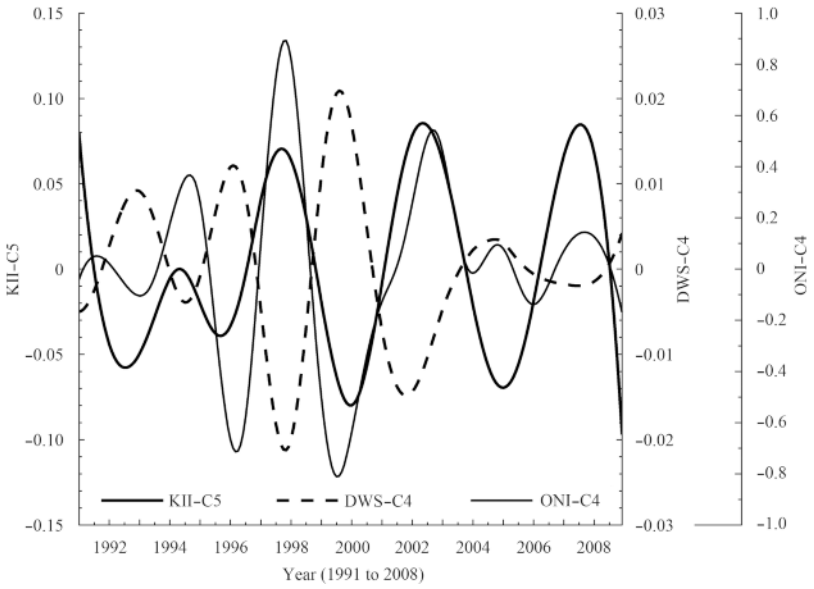

Fig. 10. Time series of the KII-C5 (bold solid curve), the DWS-C4 (dashed curve) and the ONI–C4 (thin solid curve) as shown in Figs 8 and 9.

Chen (2002) found that interannual variations of the East Asian winter and summer monsoons are closely related to El Niño and La Niña events. In the winter before the occurrence of an El Niño event, the East Asian winter monsoon is strong. When the El Niño event is developing, the East Asian summer monsoon is weak. The winter monsoon becomes weak at the mature stage of the El Niño event. When the El Niño event is decaying, the summer monsoon turns out to be strong. In contrast, a La Niña event has a similar but reverse influence on the East Asian monsoons. Based on an empirical orthogonal function analysis, Fang et al. (2006) also showed that the northeast monsoon wind weakens (intensifies) during El Niño (La Niña) events over the northern SCS. An El Niño (La Niña) event induces an anomalous lower-tropospheric anticyclone (cyclone) in the western North Pacific, resulting in a weak (strong) East Asian winter monsoon wind (Wang et al. 2000; Yuan et al., 2014). The relationship between DWS-C4 and ONI-C4 presented in Fig. 10 is consistent with these results.

The KW component mixed in the source water of the southeastern TWS actually originates from the KW intruding into the SCS through the LS. Previous investigations demonstrate that the Kuroshio intrusion is related to El Niño and La Niña events (e.g., Wu and Hsin, 2012; Yuan et al., 2014). Aside from local monsoon wind forcing, upstream Kuroshio transport also affects Kuroshio intrusion through the LS. During El Niño (La Niña) years, the bifurcation of the North Equatorial Current shifts northward (southward), which weakens (enhances) the Kuroshio transport east of the Philippines (Kim et al., 2004). Weak upstream Kuroshio transport east of Luzon results in a strong Luzon Strait transport and Kuroshio intrusion into the SCS during El Niño events, as just the opposite during La Nina events (Qu et al., 2004; Yuan et al., 2014). Wang et al. (2006) also showed that during El Niño events the intensification of remote equatorial Pacific westerly wind leads to a stronger North Equatorial Current with its bifurcation moving northward, producing a stronger transport through the LS while during La Niña events the case is reversed. They indicated that the remote wind forcing in the western and central equatorial Pacific is a dominant factor for the interannual variation of transport through the LS and the local wind forcing is secondary. Thus, more KW flows into the northeastern SCS during El Niño years than during La Niña years.

Since El Niño and La Niña events can affect both the intensity of the East Asian monsoon winds and the Kuroshio intrusion into the northeastern SCS, the synchronous change of the KII and the ONI suggests that these events also play a crucial role in the impact of KW on the source water of the northeastern TWS at the interannual time scale (Fig. 10). Recent observations also confirm this result, although they are sparse in space and sporadic in time. Shang et al. (2005) showed that an excessive intrusion of KW happened in the TWS during the 1997–1998 El Niño event as

the northeast monsoon became weak, which caused the remote sensing sea surface temperature in winter to be higher than the climatological mean value. Using observational and modeling results, Chen et al. (2010) demonstrated that little KW intruded into southern TWS during spring 2008 when a La Niña event was happening. Based on the shipboard CTD data obtained from 1991 to 2011, Huang et al. (2015) found that the salinity of seawater in the Penghu Channel, located in the southeastern TWS, is highest during El Niño events, and lowest during La Niña events.

5 Summary and conclusions

A model dataset was used to examine the impact of KW on the source water of the southeastern TWS at the seasonal and interannual timescales. To evaluate the impact objectively and quantitatively, an index (the KII) was designed with the characteristic salinity of the KW and the SCSW. The index explains the ratio of the KW in the source water, indicating the degree of impact of KW. This concept is generally accepted by oceanographers as a method of studying the mixing of different seawater masses, as well as the intrusion of one mass into another via tracers (Chen et al., 2010; Huang et al., 2015).

The impact of KW on the source water of the southeastern TWS is greater, with higher KII in winter and spring than in summer and autumn. The time-lag correlation analysis between the KII and the DWS shows that the seasonal evolution of the impact lags the wind stress by approximately two months. Northeast and southwest monsoon winds modify the SSL distribution pattern, the circulations in the northeastern SCS and the TWS, and Kuroshio intrusion through the LS. This regulates the seasonal impact of the KW on the source water.

At the interannual time scale, the KII is in phase with the ONI, but out of phase with the DWS. The impact of KW on the source water of the southeastern TWS is related to El Niño and La Niña events, as the ONI represents their emergence. The peaks of the interannual KII (KII-C5) appear in El Niño years, whereas the troughs occur in La Niña years, such as those from 1991–2008. During the El Niño events, the intensification of remote equatorial Pacific westerly wind induces a stronger North Equatorial Current with a northward shifting bifurcation than normal conditions, which produces a weaker upstream Kuroshio transport east of the Philippines and then enhances Kuroshio intrusion into the SCS; at the same time, northeast monsoon wind becomes weaker and abnormally reduces its blocking effect on the KW flowing into the southeastern TWS. As a result, more KW intrudes into the southeastern TWS. Conversely, during La Niña events, the conditions are just reversed and less KW intrudes into the southeastern TWS.

In inclusion, the impact of KW on the source water of the southeastern TWS is closely related to East Asian monsoon winds and El Niño/La Niña events. The alternation of northeast and southwest monsoon winds determines the seasonal variation of the impact by modifying the circulations in the northeastern SCS and the TWS and changing the Kuroshio intrusion through the LS. El Niño and La Niña events play an important role in the interannual variation of the impact because they affect the intensity of the East Asian monsoon winds and remote equatorial Pacific westerly wind and then the activity of the Kuroshio current.

Acknowledgements

We are thankful to Chai Fei of the University of Maine, USA who provided the modeling data used in this work as well as Xue Huijie who gave us some helpful advice on the first draft of this manuscript. Two anonymous reviewers provided some helpful suggestions for improving an earlier version of the manuscript.

References

Caruso M J, Gawarkiewicz G G, Beardsley R C. 2006. Interannual variability of the Kuroshio intrusion in the South China Sea. Journal of Oceanography, 62(4): 559–575

Chen Wen. 2002. Impacts of El Niño and La Niña on the cycle of the East Asian winter and summer monsoon. Chinese J Atmos Sci (in Chinese), 26(5): 595–610

Chen C T A, Jan S, Hsuan H T, et al. 2010. Spring of no Kuroshio intrusion in the southern Taiwan Strait. Journal of Geophysical Research, 115(C8): C08011

Chu P C, Edmons N L, Fan Chenwu. 1999. Dynamical mechanisms for the South China Sea seasonal circulation and thermohaline variabilities. Journal of Physical Oceanography, 29(1): 2971–2989

Chuang W-S. 1985. Dynamics of subtidal flow in the Taiwan Strait. Journal of the Oceanographical Society of Japan, 41(2): 65–72

Fang Guohong, Chen Haiying, Wei Zexun, et al. 2006. Trends and interannual variability of the South China Sea surface winds, surface height, and surface temperature in the recent decade. Journal of Geophysical Research, 111(C11): C11S16

Hu Jianyu, Kawamura H, Hong Huasheng, et al. 2000. A review on the currents in the South China Sea: seasonal circulation, South China Sea warm current and Kuroshio intrusion. Journal of Oceanography, 56(6): 607–624

Hu Jianyu, Kawamura H, Li Chunyan, et al. 2010. Review on current and seawater volume transport through the Taiwan Strait. Journal of Oceanography, 66(5): 591–610

Huang N E, Shen Zheng, Long S R, et al. 1998. The empirical mode decomposition and the Hilbert spectrum for nonlinear and non-stationary time series analysis. Proceedings of the Royal Society of A: Mathematical, Physical and Engineering Sciences, 454(1971): 903–995

Huang T-H, Chen C-T A, Zhang Wenzhou, et al. 2015. Varying intensity of Kuroshio intrusion into Southeast Taiwan Strait during ENSO events. Continental Shelf Research, 103: 79–87

Jan S, Sheu D D, Kuo H-M. 2006. Water mass and throughflow transport variability in the Taiwan Strait. Journal of Geophysical Research, 111(C12): C12012

Jan S, Tseng Y, Dietrich D E. 2010. Sources of water in the Taiwan Strait. Journal of Oceanography, 66(2): 211–221

Jan S, Wang J, Chern C-S, et al. 2002. Seasonal variation of the circulation in the Taiwan Strait. Journal of Marine Systems, 35(3–4): 249–268

Jia Yinglai, Liu Qinyu. 2004. Eddy shedding from the Kuroshio bend at Luzon Strait. Journal of Oceanography, 60(6): 1063–1069

Kalnay E, Kanamitsu M, Kistler R, et al. 1996. The NCEP/NCAR 40-year reanalysis project. Bulletin of the American Meteorological Society, 77(3): 437–472

Kim Y Y, Qu Tangdong, Jensen T, et al. 2004. Seasonal and interannual variations of the North Equatorial Current bifurcation in a high-resolution OGCM. Journal of Geophysical Research, 109(C3): C03040

Lai R J, Huang N. 2005. Investigation of vertical and horizontal momentum transfer in the Gulf of Mexico using empirical mode decomposition method. Journal of Physical Oceanography, 35(8): 1383–1402

Li Li, Nowlin W D Jr, Su Jilan. 1998. Anticyclonic rings from the Kuroshio in the South China Sea. Deep-Sea Research Part I, 45(9): 1469–1482

Liang W-D, Yang Y J, Tang T Y, et al. 2008. Kuroshio in the Luzon Strait. Journal of Geophysical Research, 113(C8): C08048

Nan Feng, Xue Huijie, Chai Fei, et al. 2011a. Identification of different types of Kuroshio intrusion into the South China Sea. Ocean Dynamics, 61(9): 1291–1304

Nan Feng, Xue Huijie, Chai Fei, et al. 2013. Weakening of the Kuroshio intrusion into the South China Sea over the past two decades. Journal of Climate, 26(20): 8097–8110

Nan Feng, Xue Huijie, Xiu Peng, et al. 2011b. Oceanic eddy formation and propagation southwest of Taiwan. Journal of Geophysical Research, 116(C12): C12045

Palacz A P, Xue Huijie, Armbrecht C, et al. 2011. Seasonal and interannual changes in the surface chlorophyll of the South China Sea. Journal of Geophysical Research, 116(C9): C09015

Qu Tangdong. 2000. Upper-layer circulation in the South China Sea. Journal of Physical Oceanography, 30(6): 1450–1460

Qu Tangdong, Kim Y Y, Yaremchuk M, et al. 2004. Can Luzon Strait transport play a role in conveying the impact of ENSO to the South China Sea?. Journal of Climate, 17(18): 3644–3657

Shang Shaoling, Zhang Caiyun, Hong Huasheng, et al. 2005. Hydrographic and biological changes in the Taiwan Strait during the 1997–1998 El Niño winter. Geophysical Research Letters, 32(11): L11601

Sheremet V A. 2001. Hysteresis of a western boundary current leaping across a gap. Journal of Physical Oceanography, 31(5): 1247–1259

Tsui I-F, Wu C-R. 2012. Variability analysis of Kuroshio intrusion through Luzon Strait using growing hierarchical self-organizing map. Ocean Dynamics, 62(8): 1187–1194

Wang J, Chern C-S. 1988. On the Kuroshio branch in the Taiwan Strait during wintertime. Progress in Oceanography, 21(3–4): 469–491

Wang Bin, Wu Renguang, Fu Xiouhua. 2000. Pacific-East Asian teleconnection: how does ENSO affect East Asian climate?. Journal of Climate, 13(9): 1517–1536

Wang Dongxiao, Liu Qinyan, Huang Rui Xin, et al. 2006. Interannual variability of the South China Sea throughflow inferred from wind data and an ocean data assimilation product. Geophysical Research Letters, 33(14): L14605

Wang Dongxiao, Xu Hongzhou, Lin Jing, et al. 2008. Anticyclonic eddies in the northeastern South China Sea during winter 2003/2004. Journal of Oceanography, 64(6): 925–935

Wang Xiaochun, Chao Yi. 2004. Simulated sea surface salinity variability in the tropical Pacific. Geophysical Research Letters, 31(2): L02302

Wu C-R, Hsin Y-C. 2012. The forcing mechanism leading to the Kuroshio intrusion into the South China Sea. Journal of Geophysical Research, 117(C7): C07015

Wu Zhaohua, Huang N E. 2009. Ensemble empirical mode decomposition: a noise-assisted data analysis method. Advances in Adaptive Data Analysis, 1(1): 1–41

Xiu Peng, Chai Fei, Shi Lei, et al. 2010. A census of eddy activities in the South China Sea during 1993–2007. Journal of Geophysical Research, 115(C3): C03012

Yuan Dongliang, Han Weiqing, Hu Dunxin. 2006. Surface Kuroshio path in the Luzon Strait area derived from satellite remote sensing data. Journal of Geophysical Research, 111(C11): C11007

Yuan Yaochu, Liao Guanghong, Yang Chenghao. 2008. The Kuroshio near the Luzon Strait and circulation in the northern South China Sea during August and September 1994. Journal of Oceanography, 64(5): 777–788

Yuan Yaochu, Tseng Y-H, Yang Chenghao, et al. 2014. Variation in the Kuroshio intrusion: modeling and interpretation of observations collected around the Luzon Strait from July 2009 to March 2011. Journal of Geophysical Research, 119(6): 3447–3463

Zhang Huaimin, Bates J J, Reynolds R W. 2006. Assessment of composite global sampling: sea surface wind speed. Geophysical Research Letters, 33(17): L17714

Zhuang Wei, Xie Shangping, Wang Dongxiao, et al. 2010. Intraseasonal variability in sea surface height over the South China Sea. Journal of Geophysical Research, 115(C4): C04010

Zu Tingting, Wang Dongxiao, Yan Changxiang, et al. 2013. Evolution of an anticyclonic eddy southwest of Taiwan. Ocean Dynamics, 63(5): 519–531